Vol. 13, No. 1 (2024): 278 - 287 http://dx.doi.org/10.23960/jtep-l.v13i1.278-287

JURNAL TEKNIK PERTANIAN LAMPUNG

ISSN 2302-559X (print) / 2549-0818 (online)
Journal homepage : https://jurnal.fp.unila.ac.id/index.php/JTP

The Influence of Soil Characteristic Changes on Erosion Rates Based on the Universal Soil Loss Equation (USLE) Method

Idah Andriyani[1,✉], Yaumil Zahro Fadila[1]

[1] Department of Agricultural Engineering, Faculty of Agricultural Technology, University of Jember, INDONESIA.

Article History:

Received : 09 September 2022
Revised : 09 August 2023
Accepted : 09 March 2024

Keywords:

Erodibility,
Erosion hazard level,
Nomograph,
Soil type,
USLE.

Corresponding Author:
✉ idahandriyani@unej.ac.id.
(Idah Andriyani)

ABSTRACT

Soil erodibility is a major factor contributing to soil erosion as well as the intensity of erosion rates. This study aims to validate soil erodibility values based on soil type maps through field measurements of erosion hazard level (EHL) within the Antrokan Sub-watershed area, Jember. Input data included digital maps comprising rainfall data (from 2004 to 2019), soil types, land use allocation, and Digital Elevation Model (DEM). Erosion rate was calculated using the USLE model, which was executed in two steps: (1) processing and interpreting erosion variables (R, K, LS, CP), and (2) calculating and classifying soil EHL. Field measurements indicated that soil erodibility value (K) is higher as compared to the value derived from the soil type maps. This discrepancy impacts the predicted erosion rate, where using measured K values resulted in the severe EHL category, with erosion rate of 1131 t.ha^{-1}*.y*$^{-1}$*, while using K values based on soil type maps produced erosion rate of 432.2 t.ha*$^{-1}$*.y*$^{-1}$*, categorized as moderate level. In this sense, validation of soil erodibility data is important for predicting erosion rate using USLE method. In conclusion, the soil conservation implementation to reduce K values is necessary in the Antrokan Sub-watershed area.*

1. INTRODUCTION

Soil is a fundamental natural resource extensively utilized in agriculture, serving two main functions: as a source of nutrients for plants and as a medium for anchoring plant roots. Erosion is the process of soil loss or detachment from one location, conveyed by water or wind to other locations (Saptari *et al*., 2015). The detachment, transport, and deposition of soil materials by rainfall and surface runoff explain the mechanism of soil erosion due to water. Generally, erosion is intensified by human biophysical activities or geographical conditions such as soil characteristics. Hence, research on soil characteristics and erosion rates is necessary (Shi *et al*., 2012).

Erosion measurements are commonly conducted through field observations. Field measurements to establish erosion rate with diverse land uses, soil types, and topographies, require high costs, significant labor, and relatively long time. Various erosion measurement models exist. The Universal Soil Loss Equation (USLE) is a practical model commonly employed to evaluate the rate of annual soil erosion (t.ha^{-1}.y^{-1}) for specific combinations of crop systems, management practices, soil types, rainfall patterns, and topography (Rubianca *et al*., 2018). The simplicity of the USLE can be considered advantageous, as each parameter can be studied separately to enhance transparency and objectivity of prediction results (Alewell *et al*., 2019). Moreover, the method is the most extensively used empirical model in Indonesia due to its ease of application and generality (Andriyani *et al*., 2017). The parameters utilized in the USLE method involve some factors including rainfall erosivity (R), soil erodibility (K), length and degree of land slope (LS), as well as land vegetation and conservation management practices (CP).

Many researchers have conducted soil loss studies using nomograph charts with the USLE method in the field. Cassol *et al*. (2018) correlated field-determined soil loss with rainfall erosivity and utilized the Wischmeier nomograph method to determine soil erodibility (*K*) factors in Brazil. Walker (2017) sought alternative methods to obtain equations for *K* factor in the USLE method using nomograph charts. Zhao *et al*. (2018) identified the top method to approximate *K* values and factors influencing *K* in the Ansai Watershed, Tokyo. Addis & Klik (2015) predicted spatial distributions of soil erodibility factors using USLE nomographs in the Ethiopian Watershed. Zhang *et al*. (2016) compared *K* values in agricultural soils between the US and China. El Jazouli *et al*. (2017) predicted soil erosion in the Middle Atlas Watershed (Morocco) using three different approximation including GIS (geographical information system), remote sensing, and the USLE method. Abdulkareem *et al*. (2019) predicted and assessed soil erosion influenced by land cover in the long term. Similar analyses were also conducted by Parveen & Kumar (2012) in the South Koel Basin, Jharkhand, Pham *et al*. (2018) in Central Vietnam, and López-García *et al*. (2020) in the Tzicatlacoyan region, Puebla, Mexico.

In erosion rate calculations, direct measurement of *K* values is essential to validate values derived from soil type maps. Obtaining field *K* values requires soil type data or maps in a watershed. From the soil type map, analysis of soil physical and chemical properties is conducted to obtain field *K* values. The objective of this current study is to determine the EHL (erosion hazard level) in the Antrokan Sub-watershed (Jember Regency) based on soil erodibility (*K*) values directly measured in field as well as values obtained from soil type maps.

2. RESEARCH METHOD

2.1. Location

Research was executed in the Antrokan Sub-watershed which is part of the Bedadung Watershed. The Bedadung River is one of the rivers in Jember Regency, with a length of 46.875 meters, comprising 16 Sub-watersheds, and irrigating 58.875 hectares of agricultural land (Andriyani *et al*., 2019). In recent years, the Bedadung Watershed has experienced land use changes resulting in decreased water retention capacity and increased erosion. This issue arises primarily due to extensive deforestation of woody plants surrounding the Bedadung Watershed (Andriyani *et al*., 2019), leading to environmental degradation and soil quality deterioration. Geographically, the Bedadung Watershed is located between 113˚35' to 114˚1'17" E longitude and -7˚58'8" to -8˚13'52" S latitude. Administratively, the Antrokan Sub-watershed covers an area of 1,134 ha. There are 5 rainfall stations in the Antrokan Sub-watershed, namely Kopang, Bintoro, Tegal Batu Dam, Arjasa Dam, and Manggis Dam. Sampling locations in the Antrokan Sub-watershed include upstream, middle, and downstream areas, considered representative of the research locations. The location of the Antrokan Sub-watershed within the Bedadung Watershed can be inspected in Figure 1.

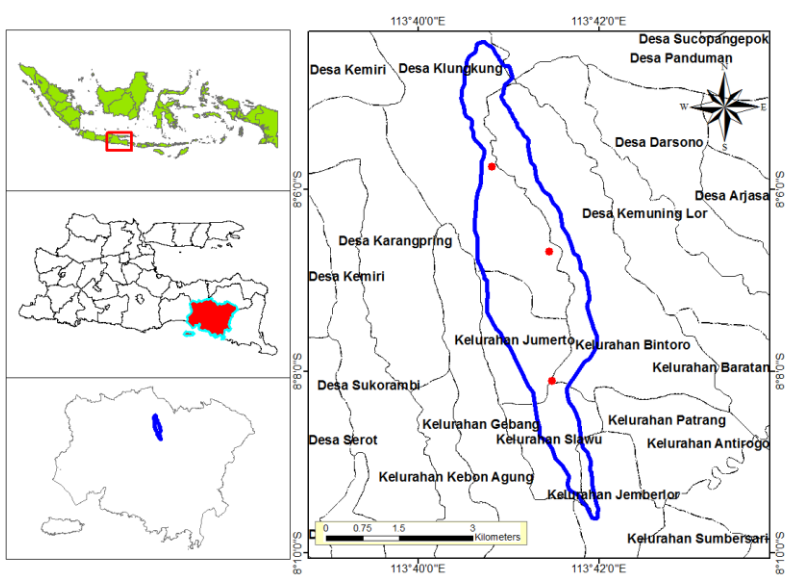

Figure 1. Research location in the Antrokan Sub-watershed, Jember Regency (red dots are sampling site)

2.2. Materials and Methods

A laptop equipped with GIS software was used in this research. The materials included annual rainfall data from 2004 to 2019 to determine the erosivity factor (*R*). Mapping of *R* values was conducted based on the site of the rainfall stations. Nomograph chart analysis and soil type maps were applied to determine the soil erodibility (*K*) factor. DEM (Digital Elevation Model) data with a resolution of 30 x 30 meters was utilized to determine the values of *LS* factor, and the 2014 RBI Map with a scale of 1:25,000 was employed to define *CP* factor. Erosion rate was approximated using the USLE method, considering the values of *R*, *K*, *LS*, and *CP* factors.

2.2.1. Data Collection and Interpretation of Erosion Factors

a. **Rainfall Erosivity Factor (*R*).** Rainfall data spanning 15 years from 2004 to 2019 were collected from 5 rainfall stations nearest to the Antrokan Sub-watershed area. The data was applied to estimate monthly *R* values (cm) based on monthly rainfall *CH* (cm) according to Equation 1 (Sulistyo, 2011):

$$R = 10.80 + 4.15CH \tag{1}$$

The erosivity values from the 5 rainfall stations were put into the rainfall station layer using GIS software. Determination of the *R* value and its spatial distribution was conducted through the Inverse Distance Weighting (IDW) interpolation.

b. **Soil Erodibility Factor (*K*)**. The method for calculating *K* values involves two approaches, namely using nomograph chart results and soil type maps. The *K* value obtained using the nomograph chart method (Figure 2) considers the portion of silt + fine sand, portions of coarse sand, soil structure, permeability, and soil organic matter. The resulting *K* values based on the nomograph chart were put into the *K* layer and then interpolated using the IDW. Soil erodibility values based on soil type maps were determined by identifying the soil types in each research location using the soil type map. The soil type was then matched with the classified *K* values as determined in Table 1. The values of *K* factor were put into the soil type layer using GIS software by converting them through "polygon to raster" tool available in the GIS software into raster format.

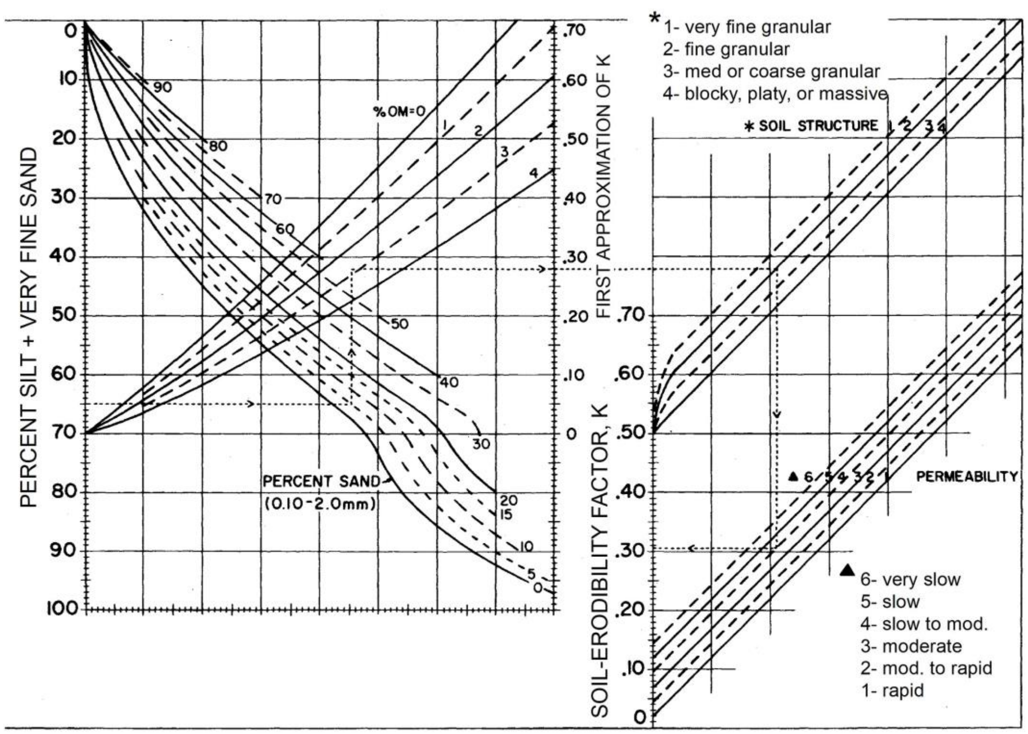

Figure 2. Nomograph chart to estimate soil erodibility (*K*) values (Corral-Pazos-de-Provens *et al*., 2023)

Table 1. Values of soil erodibility (*K*) according to soil types

No	Soil Type	K Value	No	Soil Type	K Value
1	Organic eutrophic soil	0.301	16	Blackish-gray Grumosol	0.187
2	Alluvial hydromorphic soil	0.156	17	Brown Litosol	0.175
3	Gray alluvial soil	0.259	18	Reddish-brown Latosol	0.121
4	Brownish-gray alluvial soil	0.315	19	Reddish-brown-black Latosol	0.058
5	Brownish-gray Planosol	0.251	20	Yellow-brown Latosol	0.082
6	Grey Regosol	0.304	21	Red Latosol	0.075
7	Complex of grey Regosol and Litosol	0.172	22	Yellowish-red Latosol	0.054
8	Brown Regosol	0.346	23	Complex of brown Latosol and gray Regosol	0.186
9	Brownish-yellow-brown Regosol	0.331	24	Complex of brown Latosol and yellow-brown Latosol	0.091
10	Brownish-yellow-gray Regosol	0.301	25	Complex of reddish-brown Latosol and brown Latosol	0.067
11	Complex of Regosol and Litosol	0.302	26	Complex of red Latosol, reddish-brown Latosol, and Litosol	0.062
12	Brown Andosol	0.278	27	Complex of red Latosol and reddish-brown	0.061
13	Brownish-yellow-brown Andosol	0.223	28	Complex of reddish-brown Latosol and Litosol	0.075
14	Complex of brown Andosol and brown Regosol	0.271	29	Complex of yellowish-red Latosol, reddish-brown Latosol, and Latosol	0.064
15	Gray Grumosol	0.176	30	Complex of yellowish-red Latosol, brown Latosol, reddish-yellow Podzolic soil, and Litosol	0.116

Source: Ismaniar, (2012), Taslim *et al*. (2019).

c. **Length and Degree of Land Slope Factor (*LS*)**. The values of *LS* factor was approximated using GIS software utilizing DEM (Digital Elevation Model) data that present digital surface elevations. This method was introduced by Moore and Burch in 1986 using flow accumulation and slope (Belasri & Lakhouili, 2016). The LS value was calculated as:

$$LS = \left(\frac{\gamma}{22{,}13}\right)^{0{,}4} \times \left(\frac{sin(\theta)}{0{,}0896}\right)^{1{,}3} \tag{2}$$

where γ is the slope length factor, projected horizontally (m) or (flow accumulation × cell size), and θ is the degree of land slope (= slope of DEM in degrees × 0.01745).

d. **Land Cover and Soil Conservation Factor (*CP*).** Land use types related to the *CP* factor can be reviewed from the 2014 Land Cover Map. The values of *CP* factor was defined based on the appendix of the Flood and Landslide SSOP Guidelines in 2011 by Bappenas (2012), as presented in Table 2. The *CP* factor values were put into the land use layer using GIS software. Subsequently, the land use map was converted into raster format as previously mentioned.

Table 2. Estimated *CP* factor for various land use types

No	Land Cover Type	CP	No	Land Cover Type	CP
1	Plantation	0.3	8	Settlement	1
2	Vacant Land/Grass Field	0.02	9	Rainfed Rice Fields	0.05
3	Pasture	0.28	10	Fishpond	0.001
4	Forest	0.001	11	Swamp/Mangrove Forest	0.01
5	Irrigated Rice Fields	0.02	12	Dam Lake	0.001
6	Scrubland	0.10	13	Sand	1
7	River	0.001			

Source: Bappenas (2012)

2.2.2. Prediction of Soil Erosion Rate

The estimation of soil erosion rate was performed using the USLE method, incorporating factors of *R*, *K*, *LS*, and *CP* to calculate erosion rate (*A*) according to Equation 3. The level of erosion hazard was classified into 5 levels as in Table 3.

$$A = R.K.LS.CP \tag{3}$$

where the unit of *A* is presented in $t.ha^{-1}.y^{-1}$.

Table 3. Classification of soil erosion hazard level (EHL).

No.	Erosion Hazard Level Class	Soil Loss ($t.ha^{-1}.y^{-1}$)	Classification
1.	I	< 15	Very Low
2.	II	15-60	Low
3.	III	60-180	Moderate
4.	IV	180-480	Severe
5.	V	>480	Very Severe

Source: Saiya *et al.* (2016).

3. RESULTS AND DISCUSSION

3.1. Rainfall Erosivity Factor (*R*)

The erosivity values in The Antrokan Sub-watershed indicate an average rainfall erosivity (*R*) ranging from 695 to 862 cm/year across the five stations, as shown in Figure 3*a*. High rainfall erosivity leads to the destruction of soil aggregates, resulting in pore blockage in macro pores, inhibiting water infiltration, and increasing surface runoff (Liu *et al*., 2018). The magnitude of surface runoff is influenced by topographical factors such as degree, length, and shape of land slope. Steeper slopes increase both the quantity and velocity of surface flow, enhancing the capacity to transport soil particles (Mu *et al*., 2015). With the slightly steep topography in the Antrokan Sub-watershed, the erosion potential due to rainfall also increases. The erosivity map (*R*) obtained from interpolation can be observed in Figure 3*a*.

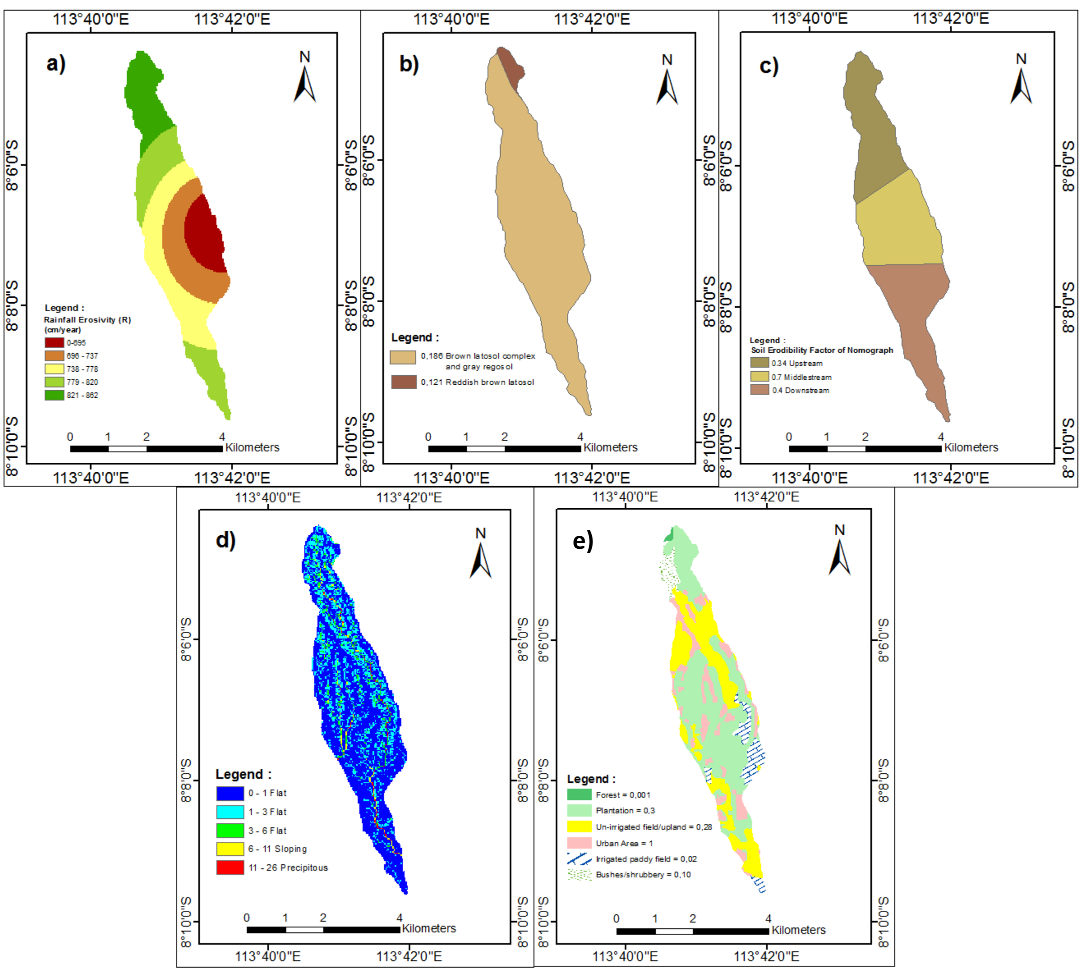

Figure 3. Maps of erosion factors: (a) Rainfall erosivity (*R*); (b) Soil erodibility based on soil map (*K*); (c) Soil erodibility based on nomograph (*K*); (d) Length and degree of land slope (*LS*); and (e) Land cover (*CP*)

3.2. Soil Erodibility Factor (*K*)

Estimation of soil erodibility factor based on field measurements combined with nomograph method results in *K* values within the Antrokan Sub-watershed as presented in Table 4. All three sampling sites have erodibility values classified as very high, likely because during laboratory analysis, fine sand and coarse sand were not separated, only total sand being analyzed. Soils having high *K* values erode more rapidly compared to those with low *K* under the same rainfall intensity (Novitasari *et al*., 2019). The measured *K* values interpolated using IDW can be observed in Figure 3*b*.

Table 4. Soil erodibility *K* values based on field measurements

No.	Soil Texture	Organic Matter (%)	Permeability (cm/h)	Soil Structure	*K* (t/ha/cm)
1	Clay	1.72	0.9766	Blocky	0.34
2	Clay loam	0.56	0.0035	Massive	0.7
3	Clay	1.59	0.0000	Massive	0.4

Table 5. Soil erodibility *K* values based on soil type maps

No.	Soil Type	*K* Value (t/ha/cm)	Erodibility Level	Area (Ha)	Area (%)
1.	Association of brown Latosol and grey Regosol	0.186	Low	38.7	77.95
2.	Reddish brown Latosol	0.121	Low	10.9	22.05

The *K* values based on soil type maps are presented in Table 5. The table points out that association of brown Latosol and grey Regosol dominate the land in the Antrokan Sub-watershed area. This soil type covering an area of 38.7 ha or 77.95% of the total area, while the rest 10.9 ha or 22.05% is covered by reddish brown Latosol. This is consistent with the results of the soil erodibility distribution map, indicating that the association of brown Latosol and grey Regosol soil type is more dominant than other soil types. Lands with soil type of the association of brown Latosol and grey Regosol have low *K* values. Areas with association of Latosol and grey Regosol soil type are more susceptible to erosion (Yuarsah *et al*., 2017). However, erosion values are not solely influenced by the *K* factor but are also affected by various factors such as slope sharpness, land cover, and rainfall intensity. The distribution map of soil types and *K* values is depicted in Figure 3*c*. The *K* values based on the nomograph are higher than those based on soil maps. This indicates an increase in *K* values, reflecting changes in soil characteristics at the research site. The *K* values are influenced by soil characteristics, namely structure, soil texture, soil organic matter, and soil permeability. The higher the *K* values, the more vulnerable the research location is to erosion.

3.3. Length and Degree of Land Slope Factor (LS)

The Antrokan Sub-watershed area is predominantly comprised by plain terrain with land slope topography of 0 - 1%, covering an area of 688.826 ha or 60.78% of the whole watershed area (Figure 3*d*). High values of *LS* factor contribute to the increase of surface runoff velocity, intensify the amount of splashed soil particles, and increase water transport energy. Aflizar *et al*. (2013) stated that during soil erosion prediction using the USLE model at a regional landscape scale, there are challenges in obtaining *LS* factors. To address this, *LS* factor calculations are grounded on raster resolution and DEM unit area. This makes it possible that the erosion prediction model to be adjusted to varying relief conditions (Kruk *et al*., 2020). The LS values within the Antrokan Sub-watershed area are presented in Table 6.

Table 6. LS factor values in the Antrokan Sub-watershed area

No.	LS Classification (%)	Area (Ha)	Area (%)
1.	0 – 1	688,826	60.78%
2.	1 – 3	324,193	28.61%
3.	3 – 6	80,787	7.13%
4.	6 – 11	29,593	2.61%
5.	<11	9,896	0.87%

Table 7. Land cover (*CP*) values in the Antrokan Sub-watershed area

No	Land Use	Area (Ha)	Area (%)	CP
1.	Forest	4.59	0.40	0.001
2.	Orchard	550.35	48.55	0.3
3.	Fallow land	304.29	26.84	0.28
4.	Settlement	149.22	13.16	1.0
5.	Irrigated rice field	83.70	7.38	0.02
6.	Shrubland	41.40	3.65	0.10

3.4. Vegetation Cover and Soil Conservation Measures (CP)

The values of *CP* factor based on land utilization in the Antrokan Sub-watershed area are presented in Figure 3*e* and Table 7. Overall, land utilization in the Antrokan Sub-watershed is dominated by orchards (48.55%), fallow land (26.84%), and settlements (13.16%) which have relatively high *CP* values. High *CP* values on a land indicate that the existing vegetation is not sufficient to control erosion. Additionally, high *CP* values indicate that no soil conservation measures have been implemented (Taslim *et al*., 2019). *CP* values approaching 0 (zero) indicate that the soil is well-protected (less sensitive to erosion). Whereas, *CP* values approaching 1 imply that the soil is freshly tilled (highly vulnerable to erosion), resulting in significant runoff (Renard *et al*., 1991). The presence of vegetation is crucial in reducing erosion rates, where the canopy can help reduce the impact of raindrops, while the roots help to bind soil and water, thereby reducing erosion rates (Taslim *et al*., 2019).

3.5. Prediction of Erosion Rate

Erosion rate was predicted using the USLE spatial-based method. The calculation process involves overlaying each erosion factor map, including maps for *R*, *K*, *CP* map, as well as *LS* within the Sub-watershed of Antrokan. Overlaying is conducted according to the soil *K* factor map resulted from the nomograph chart and soil type map. The calculation process employs raster calculator tools in GIS software. The erosion rate calculation based on soil from the nomograph chart and soil map is depicted in Table 8. Based on data in 2014, the erosion hazard level (EHL) in the Sub-watershed of Antrokan indicates severe and very severe categories. The results of the EHL also significantly differ due to the method used to estimate *K* values. Field measurement combined with the nomograph chart results in an average erosion rate of 1131 $t.ha^{-1}.y^{-1}$, whereas the *K* approximation using soil map results in erosion rate of 432.2 $t.ha^{-1}.y^{-1}$. This disparity arises due to the substantially high *K* values obtained from the nomograph chart. However, erosion rate values are also affected by some other factors including land slope and rainfall erosivity (Andriyani *et al*., 2017).

Considering the severe and very severe erosion hazard levels at the research site, conservation measures are necessary. According to (Rusdi *et al*., 2013), on lands with severe erosion hazard levels (B), efforts should focus on developing perennial crop cultivation (plantation crops or industrial crops), while lands with very severe erosion hazard levels (SB) should not be utilized for agriculture. Soil with shallow depth and steep slopes can undergo conservation practices such as continuous soil-covering crop planting. Reafforestation generally employs plants that can prevent erosion and have a long lifespan, prioritizing economically valuable hardwood plants usable for timber or by-products such as fruits, latex, roots, and oil, for example, candlenut trees and sandalwood trees. Figure 4 shows of the EHL in the Antrokan Sub-Watershed based on the nomograph chart and soil maps.

Table 8. Erosion rate in the Antrokan Sub-Watershed

No	Erosion Class ($t.ha^{-1}.y^{-1}$)	Area (ha)		Erosion Rate ($t.ha^{-1}.y^{-1}$)		Erosion Hazard Level
		Nomograph	Soil Map	Nomograph	Soil Map	
1	0 – 15	502.2	522.0	0.02	0.5	Very Low
2	15 – 60	21.2	19.0	29.9	37.4	Low
3	60 – 180	18.3	61.8	98.3	123.2	Moderate
4	180 – 480	70.8	205.7	322.0	329.1	Severe
5	> 480	509.1	308.1	2441.9	1318.9	Highly severe
	Average erosion rate ($t.ha^{-1}.y^{-1}$)			1131	432.2	

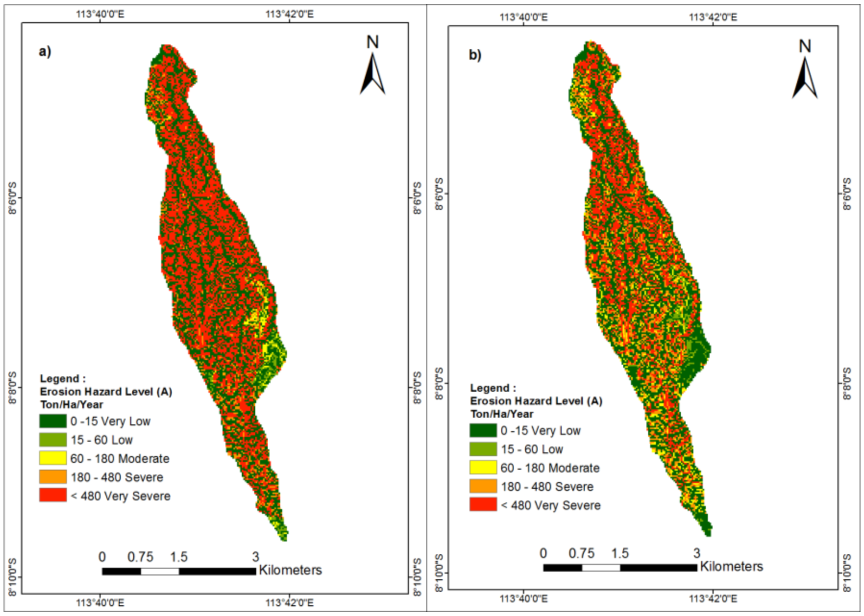

Figure 4. (a) Erosion hazard level map in the Antrokan Sub-watershed using the nomograph chart, and (b) using soil maps.

CONCLUSIONS

The values of soil erodibility (*K*) in the Sub-watershed of Antrokan based on field measurements combined with nomograph chart ranging from 0.34 to 0.7 t.ha^{-1}.y^{-1} are higher as compared to those approximated from the soil map (0.121 to 0.186 t.ha^{-1}.y^{-1}). This condition significantly affects the erosion hazard level in the prediction using the USLE model. The erosion hazard level based on field measurements falls into the category of very severe, while the erosion hazard level based on the soil map falls into the severe category. The high *K* values from field measurements may be attributed to changes in soil characteristic including soil organic matter content, soil texture, and soil permeability due to natural processes and human biophysical activities. In this sense, validation of K data is important in prediction of erosion hazard level using USLE method. Hence, conservation measures are necessary to reduce soil erodibility.

ACKNOWLEDGEMENT

Special thanks are extended to the research funding providers or donors (IsDB University of Jember 2019 Grant) and to those who assisted in the implementation of the research.

REFERENCES

Abdulkareem, J.H., Pradhan, B., Sulaiman, W.N.A., & Jamil, N.R. (2019). Prediction of spatial soil loss impacted by long-term land-use/land-cover change in a tropical watershed. *Geoscience Frontiers*, ***10***(2), 389–403. https://doi.org/10.1016/j.gsf.2017.10.010

Addis, H.K., & Klik, A. (2015). Predicting the spatial distribution of soil erodibility factor using USLE nomograph in an agricultural watershed, Ethiopia. *International Soil and Water Conservation Research*, ***3***(4), 282–290. https://doi.org/10.1016/j.iswcr.2015.11.002

Aflizar, Afrizal, R., & Masunaga, T. (2013). Assessment erosion 3D Hazard with USLE and surfer tool: A case study of sumani watershed in west sumatra indonesia. *Journal of Tropical Soils*, ***18***(1), 81–92. https://doi.org/10.5400/jts.2013.v18i1.81-92

Alewell, C., Borrelli, P., Meusburger, K., & Panagos, P. (2019). Using the USLE: Chances, challenges and limitations of soil erosion modelling. *International Soil and Water Conservation Research*, *7*(3), 203–225. https://doi.org/10.1016/j.iswcr.2019.05.004

Andriyani, I., Jourdain, D., Lidon, B., Soni, P., & Kartiwa, B. (2017). Upland farming system erosion yields and their constraints to change for sustainable agricultural conservation practices: A case study of land use and land cover (LULC) change in Indonesia. *Land Degradation and Development*, ***28***(2), 421–430. https://doi.org/10.1002/ldr.2598

Andriyani, I., Wahyuningsih, S., & Suryaningtias, S. (2019). Land use changes and its impact on erosion rates in Rembangan Sub Watershed - Jember Regency. *AgriTECH*, ***39***(2), 117. https://doi.org/10.22146/agritech.42424

Bappenas. (2012). *Analisa Perubahan Penggunaan Lahan di Ekosistem DAS dalam Menunjang Ketahanan Air dan Ketahanan Pangan.* Direktorat Kehutanan Dan Konservasi Sumber Daya Air.

Belasri, A., & Lakhouili, A. (2016). Estimation of soil erosion risk using the universal soil loss equation (USLE) and geo-information technology in Oued El Makhazine Watershed, Morocco. *Journal of Geographic Information System*, ***8***(1), 98–107. https://doi.org/10.4236/jgis.2016.81010

Cassol, E.A., da Silva, T.S., Eltz, F.L.F., & Levien, R. (2018). Soil erodibility under natural rainfall conditions as the K factor of the universal soil loss equation and application of the nomograph for a subtropical Ultisol. *Revista Brasileira de Ciencia Do Solo*, ***42***. https://doi.org/10.1590/18069657rbcs20170262

Corral-Pazos-de-Provens, E., Rapp-Arrarás, I., and Domingo-Santos, J.M. (2023). The USLE soil erodibility nomograph revisited. *International Soil and Water Conservation Research*, 11(1), 1-13. https://doi.org/10.1016/j.iswcr.2022.07.001

El Jazouli, A., Barakat, A., Ghafiri, A., El Moutaki, S., Ettaqy, A., & Khellouk, R. (2017). Soil erosion modeled with USLE, GIS, and remote sensing: a case study of Ikkour watershed in Middle Atlas (Morocco). *Geoscience Letters*, ***4***(1). https://doi.org/10.1186/s40562-017-0091-6

Kruk, E., Klapa, P., Ryczek, M., & Ostrowski, K. (2020). Influence of DEM elaboration methods on the USLE model topographical factor parameter on steep slopes. *Remote Sensing*, ***12***(21), 1–20. https://doi.org/10.3390/rs12213540

Liu, J., Wang, Z., & Li, Y. (2018). Efficacy of natural polymer derivatives on soil physical properties and erosion on an experimental loess hillslope. *International Journal of Environmental Research and Public Health*, ***15***(1), 1–14. https://doi.org/10.3390/ijerph15010009

López-García, E.M., Torres-Trejo, E., López-Reyes, L., Flores-Domínguez, Á.D., Peña-Moreno, R.D., & López-Olguín, J.F. (2020). Estimation of soil erosion using USLE and GIS in the locality of Tzicatlacoyan, Puebla, México. *Soil and Water Research*, ***15***(1), 9–17. https://doi.org/10.17221/165/2018-SWR

Mu, W., Yu, F., Li, C., Xie, Y., Tian, J., Liu, J., & Zhao, N. (2015). Effects of rainfall intensity and slope gradient on runoff and soil moisture content on different growing stages of spring maize. *Water (Switzerland)*, ***7***(6), 2990–3008. https://doi.org/10.3390/w7062990

Novitasari, N., Rohman, M.H., Ambarwati, A.A., & Indarto, I. (2019). Aplikasi USLE dan GIS untuk prediksi laju erosi di Wilayah DAS Brantas. *Jurnal Teknik Pertanian Lampung*, ***8***(2), 76–85. http://dx.doi.org/10.23960/jtep-l.v8i2.76-85

Parveen, R., & Kumar, U. (2012). Integrated approach of universal soil loss equation (USLE) and geographical information system (GIS) for soil loss risk assessment in Upper South Koel Basin, Jharkhand. *Journal of Geographic Information System*, ***4***(6), 588. http://dx.doi.org/10.4236/jgis.2012.46061

Pham, T.G., Degener, J., & Kappas, M. (2018). Integrated universal soil loss equation (USLE) and Geographical Information System (GIS) for soil erosion estimation in A Sap basin: Central Vietnam. *International Soil and Water Conservation Research*, ***6***(2), 99–110. https://doi.org/10.1016/j.iswcr.2018.01.001

Renard, K.G., Foster, G.R., Weesies, G.A., & Porter, J.P. (1991). RUSLE Revised universal soil loss equation. *Journal of Soil and Water Conservation*, ***46***(1), 30–33.

Rubianca, B., Bethanna, J., Deborah, M., & Kevin., N. (2018). A review of the (Revised) Universal Soil Loss Equation ((R)USLE): with a view to increasing its global applicability and improving soil loss estimates. *Hydrology and Earth System Sciences*, ***22***(11), 6059–6086. https://doi.org/10.5194/hess-22-6059-2018

Rusdi, R., Alibasyah, M.R., & Karim, A. (2013). Degradasi lahan akibat erosi pada areal pertanian di Kecamatan Lembah Seulawah Kabupaten Aceh Besar. *Jurnal Manajemen Sumberdaya Lahan*, ***2***(3), 240–249.

Saiya, H.G., Dibyosaputro, S. & Santosa, S.H.B. (2016). USLE Estimation for potential erosion at Wae Heu Watershed and Wae Tonahitu Watershed, Ambon Island, Indonesia. *Indonesian Journal of Geography*, ***3***(1), 56. https://doi.org/10.22146/ijg.17619

Saptari, A.S., Supriadi, A., Wikantika, K., & Darmawan, S. (2015). Remote sensing analysis in RUSLE erosion estimation. *Indonesian Journal of Geospatial,* ***4***(1), 34-45.

Shi, Z.H., Fang, N.F., Wu, F.Z., Wang, L., Yue, B.J., & Wu, G.L. (2012). Soil erosion processes and sediment sorting associated with transport mechanisms on steep slopes. *Journal of Hydrology*, ***454–455***, 123–130. https://doi.org/10.1016/j.jhydrol.2012.06.004

Sulistyo, B. (2011). Pengaruh erosivitas hujan yang diperoleh dari rumus yang berbeda terhadap pemodelan erosi berbasis raster (Studi kasus di DAS Merawu, Banjarnegara, Jawa Tengah). *Agritech*, ***31***(3), 250–259.

Taslim, R.K., Mandala, M., & Indarto, I. (2019). Prediksi erosi di Wilayah Jawa Timur. *Jurnal Ilmu Lingkungan*, ***17***(2), 323–332. https://doi.org/10.14710/jil.17.2.323-332

Walker, S.J. (2017). An alternative method for deriving a USLE nomograph K factor equation. *Conference: The 22nd International Congress on Modelling and Simulation (MODSIM2017)*, 964–970.

Yuarsah, I., Handayani, E.P., Rakhmiati, & Yatmin, . (2017). Restoration of soil physical and chemical properties of abandoned tin-mining in Bangka Belitung Islands. *Journal of Tropical Soils*, ***22***(1), 21–28. https://doi.org/10.5400/jts.2017.v22i1.21-28

Zhang, K., Lian, L., & Zhang, Z. (2016). Reliability of soil erodibility estimation in areas outside the US: a comparison of erodibility for main agricultural soils in the US and China. *Environmental Earth Sciences*, ***75***(3), 1–10. https://doi.org/10.1007/s12665-015-4980-8

Zhao, W., Wei, H., Jia, L., Daryanto, S., Zhang, X., & Liu, Y. (2018). Soil erodibility and its influencing factors on the Loess Plateau of China: A case study in the Ansai watershed. *Solid Earth*, ***9***(6), 1507–1516. https://doi.org/10.5194/se-9-1507-2018